

Article

Multi-Objective Optimisation of the Energy Performance of Lightweight Constructions Combining Evolutionary Algorithms and Life Cycle Cost

Rui Oliveira ^{1,*} , António Figueiredo ¹ , Romeu Vicente ¹ and Ricardo M. S. F. Almeida ^{2,3}

¹ RISCO-Department of Civil Engineering University of Aveiro, Campus Universitário de Santiago, 3810-193 Aveiro, Portugal; ajfigueiredo@ua.pt (A.F.); romvic@ua.pt (R.V.)

² Polytechnic Institute of Viseu, Department of Civil Engineering, Campus Politécnico, 3504-510 Viseu, Portugal; ralmeida@estv.ipv.pt

³ CONSTRUCT-LFC, Faculty of Engineering (FEUP), University of Porto, Rua Dr. Roberto Frias s/n, 4200-465 Porto, Portugal

* Correspondence: ruifoliveira@ua.pt; Tel.: +351-916-734-761

Received: 19 June 2018; Accepted: 16 July 2018; Published: 17 July 2018



Abstract: This paper discusses the thermal and energy performance of a detached lightweight building. The building was monitored with hygrothermal sensors to collect data for building energy model calibration. The calibration was performed using a dynamic simulation through EnergyPlus[®] (EP) (Version 8.5, United States Department of Energy (DOE), Washington, DC, USA) with a hybrid evolutionary algorithm to minimise the root mean square error of the differences between the predicted and real recorded data. The results attained reveal a good agreement between predicted and real data with a goodness of fit below the limits imposed by the guidelines. Then, the evolutionary algorithm was used to meet the compliance criteria defined by the Passive House standard for different regions in Portugal's mainland using different approaches in the overheating evaluation. The multi-objective optimisation was developed to study the interaction between annual heating demand and overheating rate objectives to assess their trade-offs, tracing the Pareto front solution for different climate regions throughout the whole of Portugal. However, the overheating issue is present, and numerous best solutions from multi-objective optimisation were determined, hindering the selection of a single best option. Hence, the life cycle cost of the Pareto solutions was determined, using the life cycle cost as the final criterion to single out the optimal solution or a combination of parameters.

Keywords: optimisation; evolutionary algorithms; thermal comfort; Passive House; life cycle cost

1. Introduction

The building sector represents 40% of the total European Energy balance [1]. In Portugal, the residential sector is responsible for approximately 30% of the total primary energy consumption [2]. To comply with the first Energy Performance Building Directive (EPBD) [1] requirements, new national codes were published in 2006. Following the EPBD recast publication in 2010 [1], these documents were reviewed and republished [3,4] with the goal of renovating buildings incorporating the Near Zero-Energy Building (NZEB) requirements.

The EPBD recast [1], had the ambitious goal that all new buildings should have nominal energy demands near to zero by 2020. Among the major strategies pointed out to reduce the energy consumption and greenhouse gas (GHG) emissions in the building sector [5], two key strategies

are the high performance building envelope and the use of efficient appliances (lighting, heating, cooling and ventilation). Together, these strategies form the basis of the Passive House (PH) concept. This concept is based on low energy buildings with the following premises: A well-insulated building envelope, mitigating the effects of thermal bridges to minimise possible heat losses; shape factor; efficient windows; high airtightness with controlled ventilation system with heat recovery to indirectly control condensation and mould growth associated to high moisture [6].

Combining the PH concept with renewable energy systems is a consistent pathway to more effectively attain the net zero energy buildings (ZEB) goals towards a more efficient building stock and better environment. Regarding the PH requirements, the maximum annual heating demand of $15 \text{ kW} \cdot \text{h}/(\text{m}^2 \cdot \text{a})$ (for a temperature set point of $20 \text{ }^\circ\text{C}$) or the heating load must be equal or less than $10 \text{ W} \cdot \text{m}^{-2}$; the primary energy is limited to $120 \text{ kW} \cdot \text{h}/(\text{m}^2 \cdot \text{a})$; the airtightness is restricted to 0.60 h^{-1} when a pressure difference of 50 Pa is applied (n_{50}); and thermal comfort must be met for all living areas during winter, as well as in during summer, with no more than 10% of the hours in a given year over $25 \text{ }^\circ\text{C}$ (overheating acceptable rate). To accomplish these requirements, it entails a high performance thermal envelope combined with a mechanical ventilation system with heat recovery also ensuring high indoor air quality [7].

The use of the building energy model (BEM) associated with optimisation algorithms can help in the prediction and optimisation of building performance. Several studies [8–13] showed that modelling and optimisation software (EnergyPlus, MATLAB (version R2015a, MathWorks, Natick, MA, USA), etc.) can be combined, providing designers with powerful tools to support the decision making process. According to Kämpf [14], a possible strategy involves the use of evolutionary algorithms to optimise opposite objective functions, varying parameters such as: Location and shape of buildings, technical systems, external surroundings, occupant behaviour, among others. This kind of optimisation process can be applied with feasible time resources and are useful in the design phase. These methods have been used both in residential [15–17] and service buildings [17,18].

In this paper, a hybrid evolutionary algorithm formulation designed in Reference [19] was applied to an optimisation problem. This hybrid evolutionary algorithm is based on the covariance matrix adaptation evolution strategies (CMA-ES) and hybrid differential evolution (HDE) evolutionary algorithm. HDE and CMA-ES algorithms operate in series, repeating a sequence of generations for each one algorithm until the objective function is achieved [14]. The advantage of the hybridisation of the two algorithms comes from the fact that one is best adapted to additively separable functions, and the other one to non-additively separable functions. In Figure 1, a scheme of the hybrid algorithms is presented. The hybrid evolutionary algorithm was used previously by the authors in other studies for a calibration model and energy optimisation applications using EnergyPlus [10,20–22].

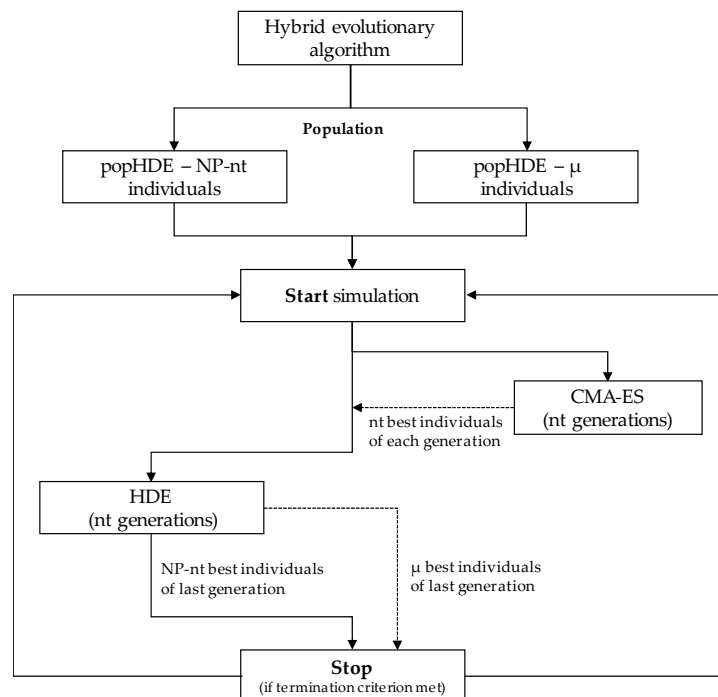


Figure 1. Scheme of covariance matrix adaptation evolution strategies (CMA-ES) and hybrid differential evolution (HDE) algorithms (adapted from Reference [19]).

In the decision-making process, the economic dimension plays a key role. One of the most well accepted methodologies to evaluate and compare rehabilitation alternatives is life cycle cost (LCC) analysis. LCC is the sum of the present value of investment and operating costs for the building and service systems, including those related to maintenance and replacement, over a specified life span. For instance, Hasan et al. [23] have used LCC, combined with simulation, on the optimisation of the U-values of typical Finnish constructions. In the context of PH design, several authors applied LCC as an optimisation criteria [24–26]. The difficulties concerning the selection of a single optimum solution after a multi-objective optimisation were discussed in Reference [27]. The authors used LCC as a final criterion in the decision-making process.

This paper is based on a lightweight building case study erected in the scope of an industrial research project “MODIKO Passive House”—in which a steel frame system was developed and optimised in order to comply with the requirements defined by the PH standard. The project included the construction of a real model in the Aveiro region (central coast of Portugal). The objective of this paper was to present and discuss the results of the optimisation procedure applied for the selection of the constructive solutions, including the adaptability of the PH standard for other climate regions of the Portuguese mainland. The combination between lightweight construction and PH design was tested, using thermal comfort, energy efficiency and LCC as performance criteria.

2. Methodology

The aim of this research was to present a methodology for the optimisation of cost effective envelope constructive solutions and heating ventilating and air conditioning (HVAC) systems to be applied to lightweight buildings in order to comply with PH comfort and energy requirements. To achieve this goal, a building energy model (BEM) was created using EnergyPlus (EP) and calibrated with monitoring data collected in situ.

The first task of the methodology was collecting temperature data from the monitoring campaign and the parameters of the real construction building to define the BEM.

Secondly, the collected data were used to calibrate and validate the BEM using a hybrid evolutionary algorithm to minimise the deviation of the Root Mean Squared Error (RMSE) between the measured and simulated indoor air temperature, suiting uncertain input parameters (design variables). The accuracy of the BEM was assessed by the goodness of fit (GOF) and Coefficient of Variation Root Mean Squared Error (CV RMSE) hourly criteria, according to the methodology proposed in [21]. The hybrid evolutionary algorithm was used to instruct the engine calculation software (EP). The calibration procedure was only carried out for Aveiro as no real data were available for the other regions. The results found in the calibration may have been different if data from a different city was used. Despite this limitation, the authors believe that using real data increases the accuracy of the model and adds value to the research.

Thirdly, the optimisation procedure was applied in six regions of Portugal: Bragança, Oporto, Aveiro, Lisbon, Évora and Faro. These locations were selected because they represent the different climatic regions of the country. The performance functions included the assessment of the indoor thermal comfort while minimising heating demand and overheating rate. The optimisation was carried out using the hybrid evolutionary algorithm for a multi-objective optimisation. The opaque constructive solutions, the windows, the air infiltration rate and the HVAC system were chosen as variables for the optimisation. The multi-objective optimisation procedure provided the Pareto front of optimum solutions. In Section 5, the multi-objective optimisation using evolutionary algorithm is presented in detail. For each optimisation, a total of 10,000 simulations were carried out. The optimisation was performed using a server with Intel Core i7 5820K with six dedicated cores working at 3.3 GHz.

Finally, an economic analysis based on the LCC was implemented for the selection of the optimum solutions based on the multi-objective optimisation. This methodology is depicted in Figure 2.

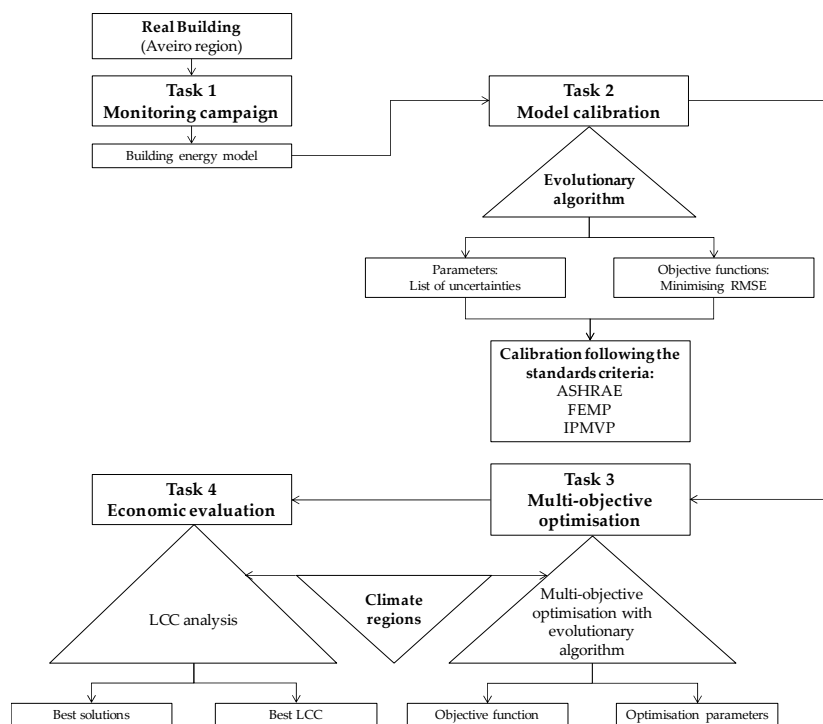


Figure 2. Methodology: Monitoring, model calibration, multi-objective optimisation and life cycle cost (LCC) evaluation.

3. Building Data Collection

3.1. Building Location and General Characterisation

The building used as case study was built in 2015 in a suburban area of the city of Aveiro on the north coast of Portugal mainland (latitude $40^{\circ}60'$, longitude $8^{\circ}60'$) about 15 km away from the Atlantic coast and 50 m above sea level. The building had a contemporary architecture design inserted in a residential area with one family dwelling buildings of similar geometry, as displayed in Figure 3.



Figure 3. Case study: (a) northeast external wall; (b) southwest external wall.

The one-family building had two floors and a steel structure, shown in Figure 4. The building had 148 m^2 of treated floor area and 318 m^2 of exterior surface area, of which 198.4 m^2 were opaque external wall. The glazing to wall ratio was 15.4%, approximately. This ratio was quite different for the four external walls, with a ratio of 26% in the north and 60% in the south external wall. To prevent overheating, a shading overhang and external venetian shutters were installed in the south-oriented windows as shading devices.

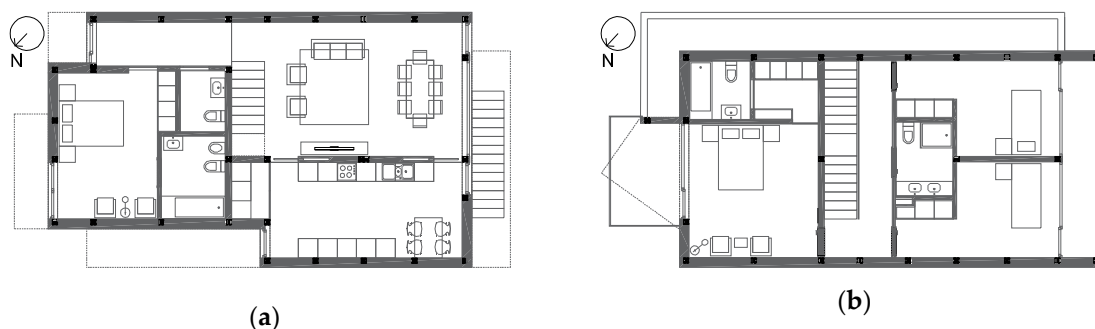
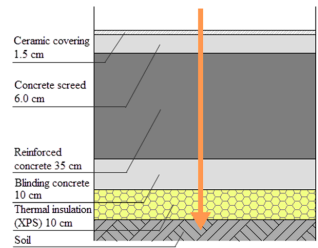
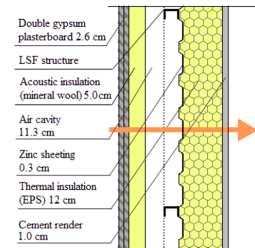
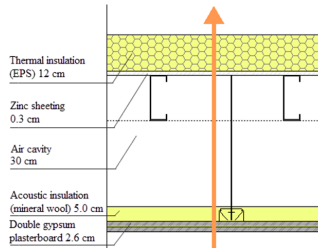


Figure 4. Architectural drawings of the building: (a) ground floor; (b) first floor.

The building structure was founded on a massive ground floor concrete slab with thermal insulation underneath which supported the cold formed steel structure. The exterior wall panels consisted of a thick thermal insulation layer assembled with a secondary steel structure. The flat roof was composed of thermal insulation panels fixed to zinc sheeting over the main steel structure. The constructive solutions are displayed in Table 1, including the corresponding U -values.

Table 1. Constructive solutions of the opaque building envelope.

Ground Floor Slab	External Walls	Flat Roof
		
$U_{value} = 0.32 \text{ W}/(\text{m}^2 \cdot ^\circ\text{C})$	$U_{value} = 0.21 \text{ W}/(\text{m}^2 \cdot ^\circ\text{C})$	$U_{value} = 0.21 \text{ W}/(\text{m}^2 \cdot ^\circ\text{C})$

The linear thermal bridges were analysed in accordance with EN ISO 10211:2007 [28] and all comply with the $\Psi_{value} \leq 0.01 \text{ W}/(\text{m}^2 \cdot ^\circ\text{C})$ required by PH.

The thermal properties of the windows and doors were: Thermal transmission coefficient $U_{w,installed} = 1.72 \text{ W}/(\text{m}^2 \cdot ^\circ\text{C})$ and $U_{w,installed} = 1.69 \text{ W}/(\text{m}^2 \cdot ^\circ\text{C})$ for the north and south windows, respectively; solar heat gain coefficient (SHGC) = 0.57; and external doors $U_{w,installed} = 1.90 \text{ W}/(\text{m}^2 \cdot ^\circ\text{C})$. These values take into account the frame (U_f) and glass edge thermal bridge (Ψ_g) in accordance with ISO 10077 [29] and the thermal bridge due to installation ($\Psi_{Install}$) in accordance with EN ISO 10211 [28].

For the HVAC system, a compact heat pump unit was chosen, incorporating: Ventilation and passive recovery unit, as well as a supplementary energy efficient heating system, to offset the air temperature when the heat exchanger cross flow is not sufficient.

3.2. Weather Files Considered for BEM

The World Map of Köppen-Geiger Climate Classification [30] establishes an organisation of the world map classified in five main climates. Portugal is assembled in the Csa (south of the country) and Csb (centre and north of the country) regions. In this study, six locations were selected, representative of different winter and summer conditions and severity, which together characterise the climatic regions of the country, shown in Figure 5. Bragança and Évora are representative of the north and south interior, respectively. Oporto, Lisbon and Faro represent the north, centre and south coast of Portugal's mainland, respectively. Aveiro is the location of the case study.

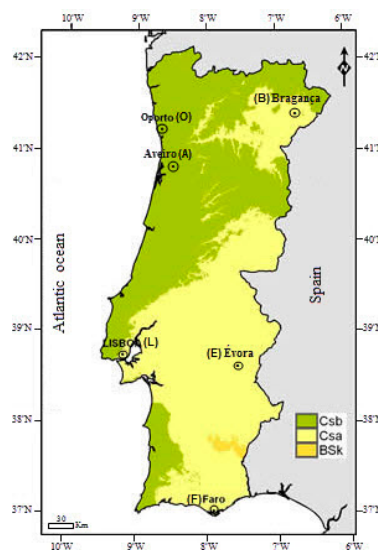


Figure 5. Portugal mainland: Six regions under study (Source: Adapted from Reference [31]).

The weather files for these regions were obtained from the National Laboratory for Energy and Geology (LNEG) [32]. The files were built from weather data collected by the Portuguese Sea and Atmosphere Institute (IPMA) using measurements carried out between 1971 and 2000. The weather data of the regions used in the simulations are summarised in Figures 6 and 7.

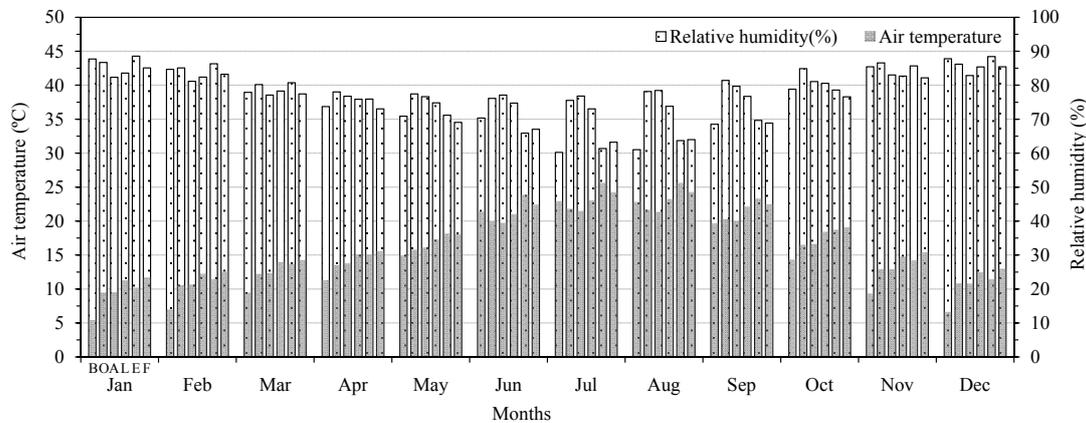


Figure 6. Weather data for the six locations (source: [32]): Average monthly air temperature and relative humidity. Nomenclature: B—Bragança; O—Oporto; A—Aveiro; L—Lisbon; E—Évora; F—Faro.

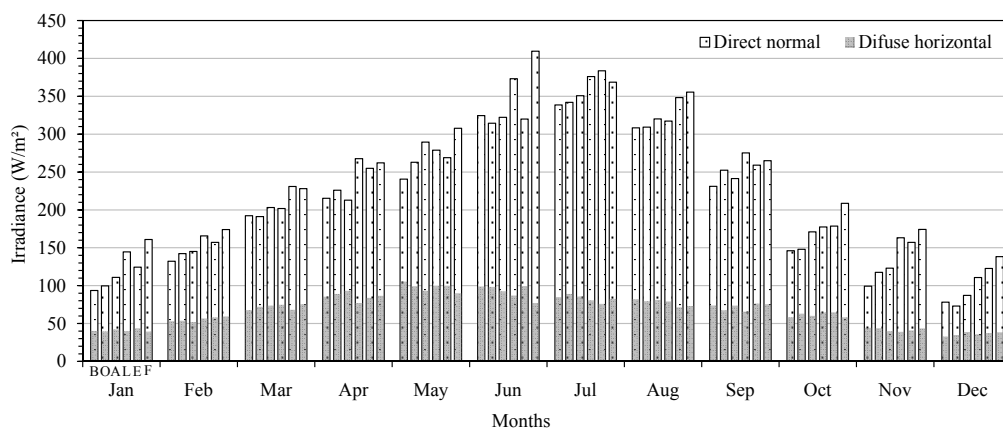


Figure 7. Weather data for the six locations (source [32]): Average monthly solar irradiance, direct normal and diffuse horizontal irradiance. Nomenclature: B—Bragança; O—Oporto; A—Aveiro; L—Lisbon; E—Évora; F—Faro.

Figures 6 and 7 show that for all regions the months with both the highest temperatures and highest irradiances occur from June to August with the lowest relative humidity. Évora and Faro represent the hottest regions of the country. The lowest temperature and irradiance occur from December to February, with the highest relative humidity. Bragança, Oporto and Aveiro, located in north of the country, have more severe winter conditions. The locations with higher solar irradiance are Lisbon and Faro, both on the coastline.

3.3. Monitoring of the Building

The real data collected during the hygrothermal monitoring campaign were fundamental to achieving an accurate BEM. To that the end, thermo-hygrometer sensors were installed in six compartments to record the air temperature and relative humidity. The temperature probe had an accuracy of 0.5 °C and a resolution of 0.1 °C while the humidity probe had an accuracy of 3% and a resolution of 0.1%. The building was monitored from the 22 October 2017 to 21 December 2017. The sensor's positions inside the compartments were chosen in order to avoid direct sun exposure

from the glazed areas. The monitoring acquisition system was logged at 10-minute intervals and averaged hourly. The sensors were distributed in accordance with ISO 7726 recommendations [33], positioned approximately at a 1-m height. Figure 8 shows the position of the thermo-hygrometer (TH) sensors in the compartments.

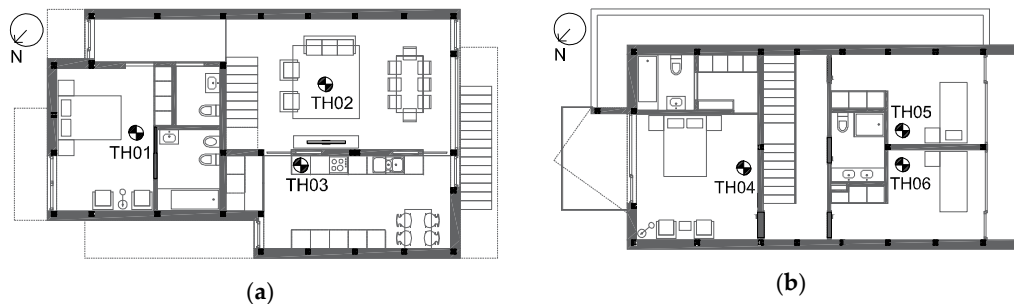


Figure 8. Identification and location of the sensors: (a) ground floor; (b) first floor.

The exterior dry bulb temperature, relative humidity, solar irradiation, and wind speed and direction were collected from a nearby weather station and used in the BEM for calibration purposes. Direct and diffuse irradiance were converted from the monitored global horizontal solar radiance using the operational model developed by Cipriano et al. [34].

Figure 9 presents the variation in the air temperature in the six compartments and in the exterior during the monitoring period. These results show that the indoor temperature practically complies with the thermal comfort range (20–25 °C) established by PH requirements during almost the entire period.

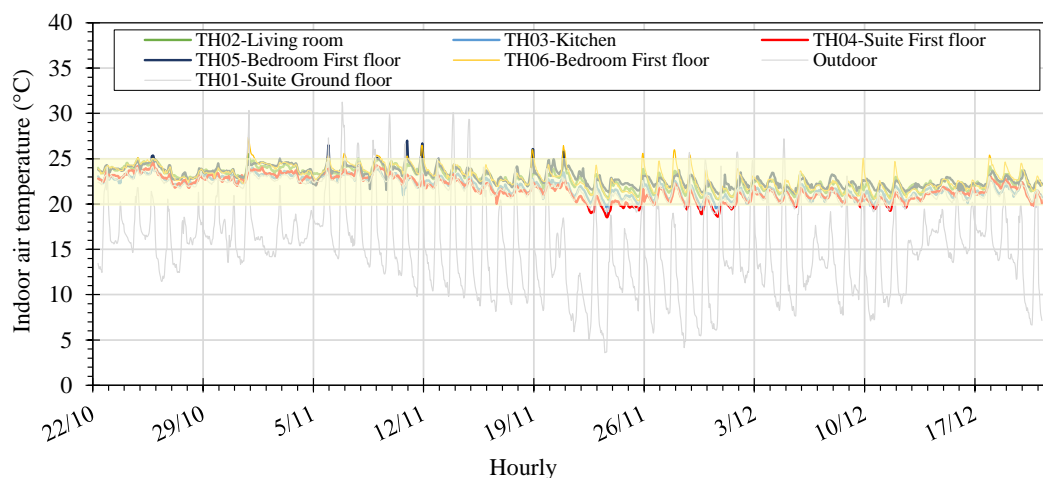


Figure 9. Indoor and outdoor air temperature from monitoring.

The air infiltration was evaluated by a blower door test, shown in Figure 10a. The air change rate at a pressure difference of 50 Pa (n_{50}) was 0.9 h^{-1} which indicates a very airtight building envelope and represents 10% below the limit value of 1.0 h^{-1} required by the PH standard for European warm climates, as presented in the Passive-On [35] study.

The air change rate (ACR) due to the Mechanical Ventilation with Heat Recovery (MVHR) system was evaluated with discrete measurements of the air velocity at the ventilation grids of each compartment, shown in Figure 10b. The air velocity was logged with an anemometer with an accuracy of 0.2 m/s and a measuring range of 0.6 to 40 m/s . In each compartment, the final velocity was the average of nine points around the ventilation grids in accordance with Reference [36], as illustrated in Figure 10c.

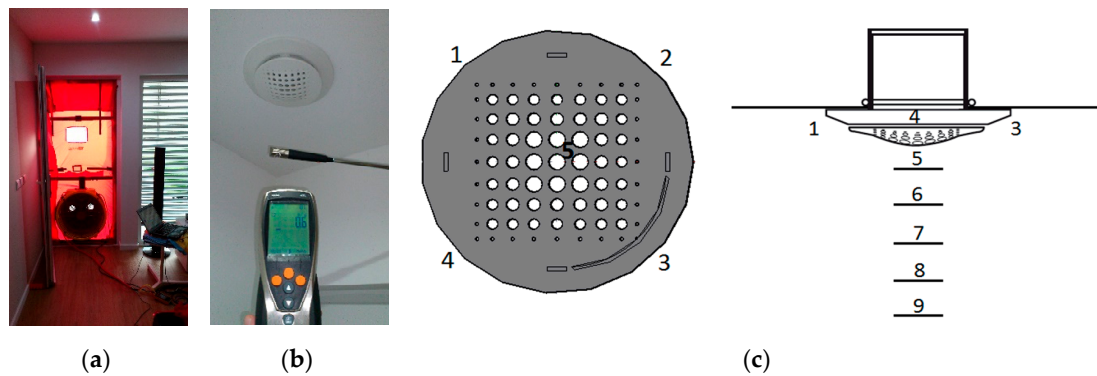


Figure 10. Experimental ventilation campaign: (a) blower door test setup; (b) air velocity measured with the anemometer probe; (c) measuring points.

3.4. Numerical Model Definition

Based on the parameters defined in the previous sections (3.1–3.3), a dynamic thermal simulation model was created in OpenStudio[®] (Version 2.6.0, National Renewable Energy Laboratory, Golden, CO, USA) to be simulated in EnergyPlus[®] software. Figure 11 presents the Northeast and Southwest views of the BEM designed through the SketchUp[®] and OpenStudio[®] plug-in where the adjacent constraints were included in the BEM geometry as shading surfaces. A complete description of the BEM can be found in [20]. The model includes nine thermal zones (TZ), corresponding to the internal compartments of the building, shown in Figure 11. Thermal zone TZ01—Living room, which includes the hall and the staircase, establishes the connection with the elevated floor and thus is considered in both. The remaining TZ are as follows: TZ02—kitchen; TZ03—ground floor suite bedroom; TZ04—ground floor bathroom; TZ05—first floor suite bedroom; TZ06—first floor bathroom and TZ07/TZ08—first floor single room.

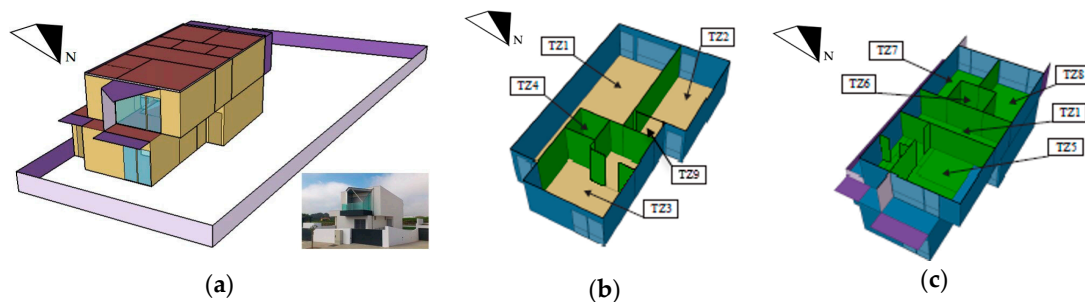


Figure 11. 3D model definition: (a) Building energy model geometry; (b) thermal zones division—ground floor; (c) thermal zones division—first floor.

Real schedules were defined for the occupancy, equipment, electric devices and artificial lighting hours. The building was occupied by a family composed by two adults and two children (100% of occupation level/density) and the schedule routine was based on the behaviour of the residents, as presented in Table 2. During the remaining hours the zones were unoccupied. The remaining internal gains (lighting and electric equipment) were included in the model, also in accordance with real schedules provided by users.

Table 2. Occupancy schedule of relevant thermal zones TZ0#.

Thermal Zone	Level * (%)	Profile		
		Week Day	Weekend	
TZ01	25	On From	15:00 to 16:00	-
	50		18:00 to 20:00	22:00 to 24:00
	100		20:00 to 22:00	14:00 to 21:00
	25		22:00 to 23:00	-
TZ02	25	On From	7:00 to 8:00	7:00 to 8:00
	50		15:00 to 16:00	15:00 to 16:00
	50		19:00 to 20:00	19:00 to 20:00
TZ03/TZ05/TZ07/TZ08	100		00:00 to 8:00	00:00 to 8:00
	100		21:00 to 24:00	21:00 to 24:00

* 100% represents 4 occupants.

The MVHR was always in operation to guarantee adequate indoor air quality and thermal comfort. During the monitored period, the external venetian shading devices were manually controlled by the occupants. Once again, the shading device's schedule was defined according to the occupants' behaviour: (i) closed—from 18:00 to 8:00 and (ii) open—from 8:00 to 18:00.

4. Model Calibration

4.1. Definition of the Unknown Parameters

In the first step of the model calibration, 15 input parameters (x_0 to x_{14}) were identified as the ones with the highest uncertainty. Consequently, a range of variation was defined for each one, presented in Table 3. Parameters x_0 to x_3 (insulation thickness) were selected as uncertainty variables to take into account the thermal bridge's impact and, therefore, their range of variation is rather narrow. Parameters x_4 and x_5 are related to the exterior windows U_{value} coefficient, with a range limit (5%) of the value given by window manufacturer. Parameter x_6 (n_{50}) has a significant impact on the indoor air temperatures, as well as on the space heating or cooling energy needs in buildings. The range defined (0.3 to 1.5 h^{-1}) was based on a blower door test carried out with a 50 Pa pressure difference. Parameters from x_7 to x_{14} represent the air change rate (m^3/h) provided by the mechanical ventilation system. The ACR was directly evaluated from the ventilation grids using different parameters divided by thermal zone. All uncertainties were considered as continuous variables with the box constraint limits defined in Table 3.

Table 3. Range of the unknown input parameters (continuous variables).

Parameter id.	Designation (Units)	Box Constraints Limits
x_0	Ground floor insulation thickness (m)	0.080–0.100
x_1	External wall insulation thickness (m)	0.114–0.120
x_2	Roof insulation thickness—Ground floor level (m)	0.160–0.180
x_3	Roof insulation thickness—First floor level (m)	0.130–0.150
x_4	North windows: U_{value} ($\text{W}/\text{m}^2\cdot^\circ\text{C}$)	1.634–1.806
x_5	South windows: U_{value} ($\text{W}/\text{m}^2\cdot^\circ\text{C}$)	1.606–1.775
x_6	Infiltration rate at 50 Pa (h^{-1})	0.300–1.500
x_7 – x_{14} (by thermal zone)	Air change rate (m^3/h)	2.700–70.540

4.2. Accuracy Criteria for the Building Energy Model

The model was validated according to the criteria (or the limit values) defined by the following standards: (i) American Society of Heating, Refrigerating and Air-Conditioning Engineers (ASHRAE) guideline 14 [37], (ii) the International Performance Measurement and Verification Protocol (IPMVP) [38] and (iii) the Federal Energy Management Program (FEMP) [39].

The strategy used to calibrate the model consists of achieving the best match between measured and simulated indoor air temperatures. For the BEM calibration, two indexes were evaluated to assess the model's accuracy: (1) normalised mean bias error (NMBE) and (2) coefficient-of-variation of the root mean square error (CV RMSE). The assumption of standardised statistical indexes is proposed by the authors in Reference [40] to represent the performance of a model defined in References [40–42].

The NMBE index establishes the fit of the simulated and monitored data. NMBE is defined by Equation (1) and calculated as the sum of errors between the measured and simulated data for each timestep (hourly data) of the considered period.

$$\text{MBE} = \frac{\sum_{i=1}^n (M_i - S_i)}{n \times \overline{M}_i} \times 100 \quad (1)$$

The calibration process, according to the methodology proposed, defines the root mean square (RMSE) coefficient as the objective function in the evolutionary algorithm, which establishes the basis to CV RMSE evaluation. The RMSE is a measure of the variability of the data defined by Equation (2). The difference in paired data points is calculated and squared hourly.

$$\text{RMSE} = \sqrt{\frac{1}{n} \sum_{i=1}^n (M_i - S_i)^2} \quad (2)$$

The CV RMSE index enables the determination of how well a model fits the data by capturing offsetting errors between measured and simulated data and acting as a measure of the GOF index. The CV RMSE index is calculated using Equation (3):

$$\text{CV RMSE} = \frac{\sqrt{\frac{1}{n} \sum_{i=1}^n (M_i - S_i)^2}}{\overline{M}_i} \times 100 \quad (3)$$

In this equation, M_i is the measured data and S_i is the simulated data for the time i , which refers to the hour of the day. The \overline{M}_i is the average value of the measured data points for the considered period n (hourly).

The GOF and CV RMSE indexes were the selected criteria to validate the model's accuracy. A consolidated way to define an index based on NMBE and CVRMSE is to calculate GOF. The GOF index is determined by Equation (4):

$$\text{GOF} (\%) = \frac{\sqrt{2}}{2} \times \sqrt{\text{NMBE}^2 + \text{CV RMSE}^2} \quad (4)$$

4.3. Evaluation of the Calibration Procedure

The EnergyPlus outputs were programmed using the Energy Management System (EMS) application to calculate the RMSE index. Then, the evolutionary algorithm was used to minimise the objective function (RMSE index) aimed at finding a trade-off between the input design parameters (defined as variables in Table 3) according to monitored indoor air temperatures. Figure 12a shows the coefficient of determination (r^2) between the real data and simulated results derived from the best id. attained. The optimal solution is shown in Figure 12b. For temperatures between 20 °C and 22 °C, the deviation between simulated results and monitored data reveals a tendency of higher temperatures for the monitored data. From 22 °C to 24 °C, the observed deviation can be considered well fit, with small discrepancies in this range. In an overall analysis, the coefficient of determination of 0.99 reveals the accuracy of model-fitting.

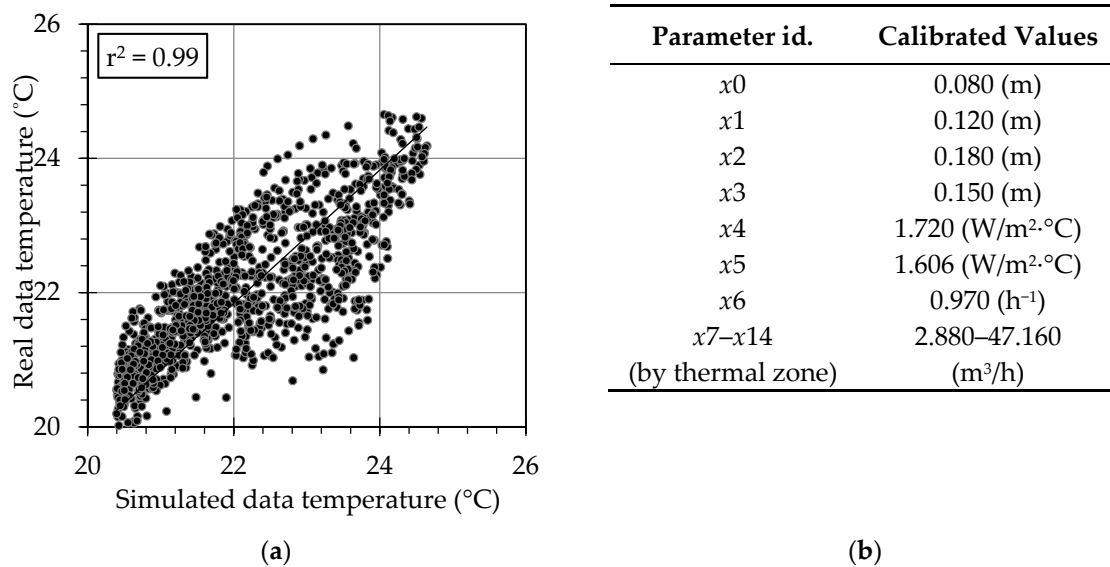


Figure 12. Best model results for period under calibration—id. 10298: (a) index and correlation factor; (b) calibrated values.

The CV RMSE values attained, shown in Table 4, are below the limit values imposed in the ASHRAE Guidelines [37], the IPMVP [38] and the FEMP [39] standards. The validation of the BEM follows the criteria of these standards, as shown in Table 4. According to the GOF index, ASHRAE Guidelines recommend a GOF below 11% and Cipriano et al. [34] suggests a GOF below 3% for trial's acceptance. In the presented work, the attained GOF is lower than the values suggested. In this study the three guidelines identified were verified, meaning that there is an acceptable agreement between measured and simulated data.

Table 4. Acceptance criteria used for building energy model (BEM) calibration—id. 10298.

Calibration Results—id# 10298				Hourly Criteria (%)	
NMBE	RMSE	CV RMSE	GOF	Standards	CV RMSE Limits
-0.65	0.72	3.28	2.36	ASHRAE Guideline	30
				IPMVP	20
				FEMP	30

5. Passive House Optimisation for Different Regions

5.1. Multi-Objective Optimisation Using Evolutionary Algorithm

Finding the best design solution for a PH building is a complex problem in the sense that there are several good solutions resulting from the combination of parameters which satisfy the energy demand limits and comfort requirements. Thus, the use of evolutionary algorithms with multiple conflicting objectives could be a possible tool to use for assessing design actions.

The optimisation process starts from the calibrated model described in the previous section, followed by the multi-objective optimisation process using the hybrid evolutionary algorithm to develop the optimised BEMs.

The objective functions are the goals of the optimisation process and are discussed in Section 5.2. The calculation of the objective functions was performed using the Energy Management System (EMS) application of EnergyPlus[®]. The hybrid evolutionary algorithm was used to instruct the energy simulation program and to select a set of optimised alternatives.

A multi-objective optimisation process, to optimise buildings parameters, involves identifying the optimisation parameters: envelope solutions and control systems features presented and discussed in Section 5.3.

After optimisation parameter analysis and the objectives function calculation process mentioned above, the detailed implementation of the multi-objective optimisation process using an evolutionary algorithm for solving BEM problem was performed. Finally, results generated after the multi-objective optimisation process can be reported using the Pareto-optimal fronts indicating all non-dominated solutions. These results are presented in Section 5.4.

For a thorough understanding of the whole process of the multi-objective optimisation, a workflow is summarised in Figure 13.

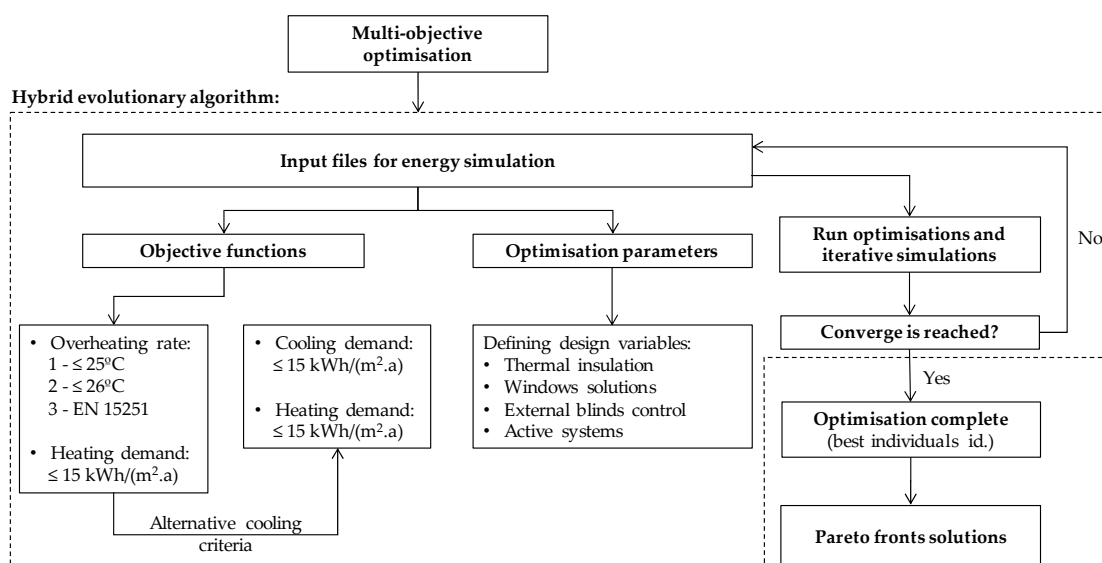


Figure 13. Multi-objective optimisation process.

5.2. Objective Functions

The overheating rate (with a maximum limit of 10%) and heating demand (with a maximum limit of $15 \text{ kW}\cdot\text{h}/(\text{m}^2\cdot\text{a})$) were settled as the objective functions (PH compliance criteria).

The overheating rate is the sum of the discomfort time for the entire building according to the PH requirements and to EN 15251 [43] for category II relative to a normal comfort level adjusted for new buildings. The 25°C limit is defined by the PH standard, however a more permissible limit of 26°C was also evaluated taking into account the warm climate context. The overheating rate upper limit established by the adaptive comfort analysis of the EN 15251 was the third criteria chosen. In a second approach for the climatic regions where the overheating rate criteria is not fulfilled, an alternative cooling criterion was tested, adding a cooling unit into the model. In these cases, the cooling demand (with a maximum limit of $15 \text{ kW}\cdot\text{h}/(\text{m}^2\cdot\text{a})$) was used as an objective function.

5.3. Optimisation Parameters

In the optimisation process, the identification of the parameters in use puts forward a set of alternative measures for building design. Table 5 presents the list of parameters for the input database.

The minimum of the reference parameters (U_{value} for opaque and translucent surfaces) was defined from Portuguese standards (REH) [3]. In the BEM, a schedule was created to control the blinds activation (automatic shading device with horizontal slats regulated between 5° to 90°) in the summer season triggered by indoor air temperature values. The shading system used allows for the possibility to achieve the optimal activation temperature for each climate region studied, also including optimisation of the slat angle of the blinds. The external blinds worked in automatic mode from the

1 June to 31 October. The parameters used in the optimiser are presented in Table 5, as well as the box constraints.

Table 5. List of parameters in action (continuous variables).

Parameter id.	Designation	Box Constraints
#00	Pavement insulation thickness (m)	0.060–0.240
#01	Wall insulation thickness (m)	0.020–0.240
#02	Roof insulation thickness (m)	0.040–0.300
#03	Exterior windows North (-)	Defined as discrete variables (Table 6)
#04	Exterior windows South (-)	
#05	Blinds: slat angle (°)	5.000–90.00
#06	Blinds: activation by temperature (°C)	≥21.00
#07	Bypass: air flow rate (h ⁻¹)	0.000–1.800
#08	Bypass: activation temperature (°C)	21.00–26.00
#09 to #16 (by thermal zone)	Air change rate (h ⁻¹)	0.300–0.600
#17	Activate system solution	Defined as discrete variable

Two different pieces of mechanical equipment for heating and ventilation were combined as a discrete variable to simulate two scenarios: (i) traditional HVAC system and (ii) heat pump unit with heat recovery ventilation (MVHR). The MVHR is an essential component to achieve the PH requirements, however, in some regions their use could be unnecessary. This conclusion was presented in [20], which defined that the heat recovery feature of the mechanical ventilation system may not be necessary in regions with low heating demand, such as the southern regions of the Portuguese mainland.

The parameters defined for each region were combined with six different windows solutions, shown in Table 6, integrated as a discrete variable in the optimisation process. These solutions resulted from a survey on the typical solutions used in southern Europe. The data for this survey were collected from manufacturers with windows expertise.

Table 6. Windows solutions (discrete variables).

Solution (S_i)	S1	S2	S3	S4	S5	S6
Glazing Type	Double Glazing			Triple Glazing		
U_f	1.50	1.50	1.50	1.50	1.50	1.10
U_g	1.40	1.40	1.50	1.40	1.40	0.60
SHGC	0.38	0.48	0.57	0.62	0.71	0.54

SHGC—Solar Heat Gain Coefficient.

5.4. Numerical Results

The results are presented as a Pareto front, which represents the optimal set of solutions after 10,000 runs for each region. Pareto fronts are frequently used for analysing BEM optimisation results with multi-objective solutions, defining a set of design solutions as an optimal solution set. For these possible solutions, a unique situation occurs where a single objective adversely affects other objectives [44].

The PH features optimisation, shown in Tables 5 and 6, for different climate regions in the Portuguese mainland were performed and are displayed as data plots shown in Figure 14. The weather files used for each region were presented in detail in Section 3.2. Building stakeholders can assess the trade-offs between optimised design solutions of the Pareto front for three comfort criteria defined and referred to in Section 5.3.

The multi-optimisation was computed, defining the optimum constructive solutions to fulfil the PH requirements, shown in Figure 14. The results show an exceedance of the overheating risk rate when considering the EN15251 standard approach. For the others approaches, and considering the

maximum admissible value of 10% for the overheating risk, an active cooling system is needed for air conditioning, excluding the Oporto and Aveiro regions, shown in Figure 14a,d, respectively, where the indoor air temperatures are lowest.

Oporto, Aveiro, Lisbon, Évora and Faro, characterised by moderate temperatures felt during the winter season, provide an easy way to comply with the heating demand limit for the criteria under study. For Bragança, the heating demand is higher, which is characterised by a more severe winter, however, the heating demand limit was accomplished. Figure 14 presents the Pareto front results for the three comfort criteria defined in Section 5.3 associated with the overheating rate and cooling demand limit. These results, which are severely influenced by the weather location conditions, are in line with others research studies presented in References [10,45].

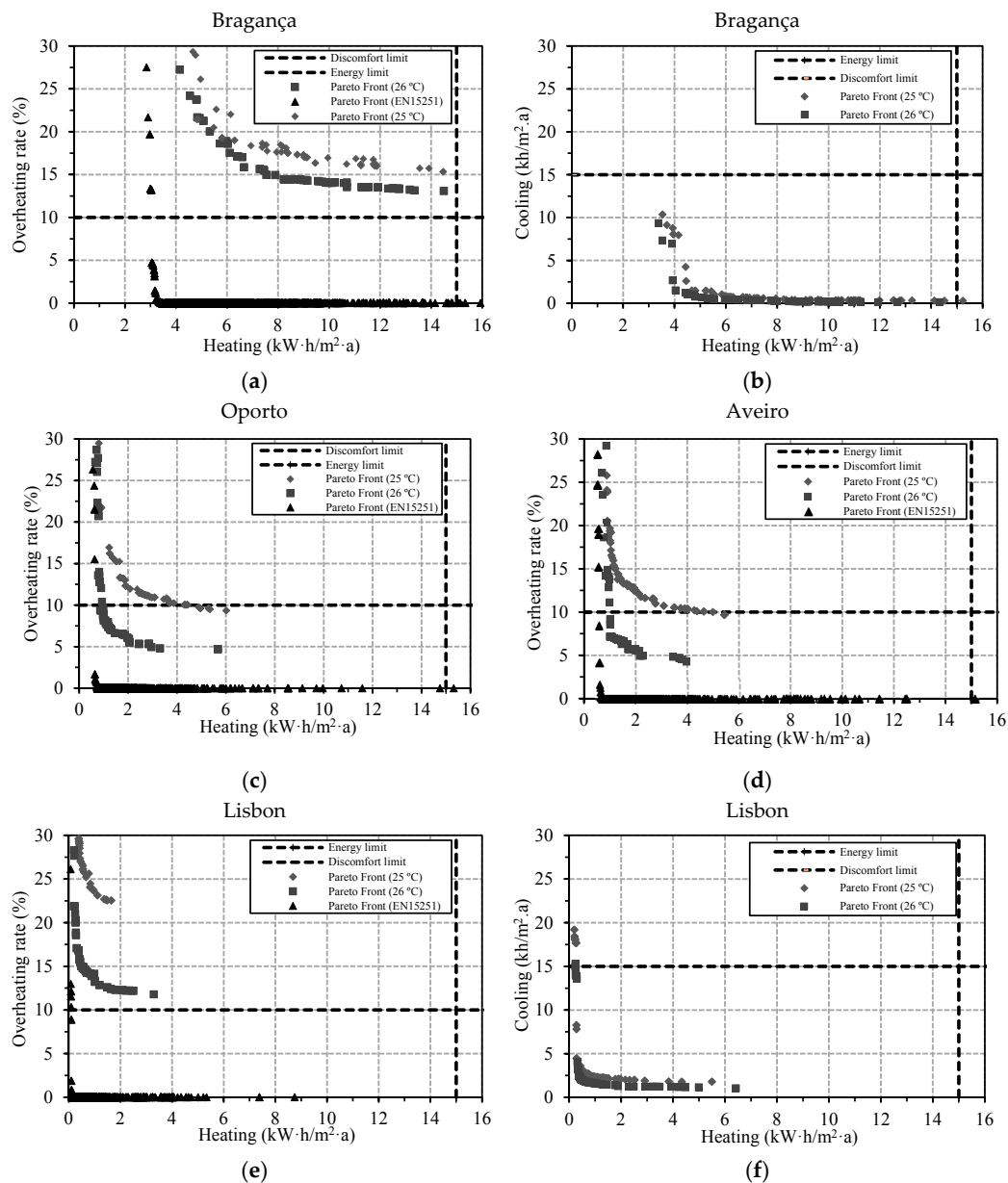


Figure 14. Cont.

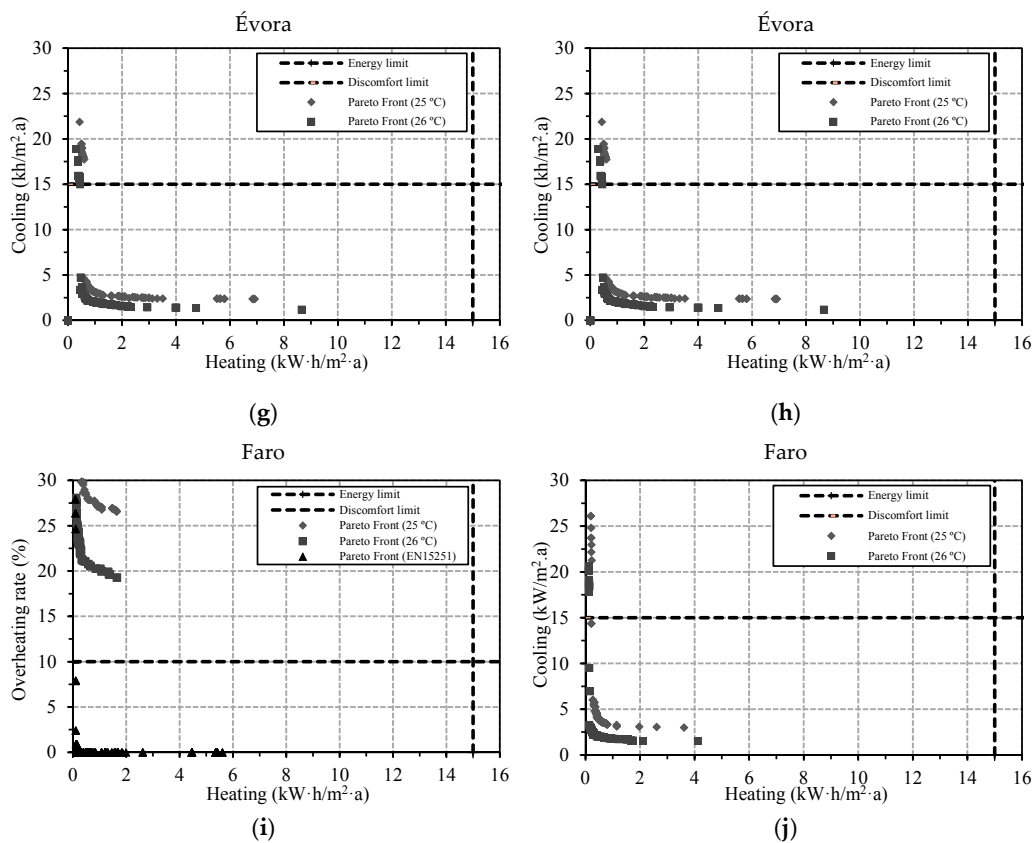


Figure 14. Pareto front results for all regions: (a,c–e,g,i) heating vs. overheating rate; (b,f,h,j) heating vs. cooling.

5.5. Discussion

In summary, these results suggest that using the EN 15251 criteria, the PH requirement for both limits was easily achieved for all climate regions. Moreover, the majority of the scenarios in the Pareto front accomplish the heating demand.

For the overheating rate limits, considering the 25 °C and 26 °C maximum temperature criteria, the PH requirements were achieved only for the Oporto and Aveiro regions. Thus, an active cooling system was needed to reduce the overheating rate for the other climate regions under study. The use of an active system allows the compliance of the cooling demand criteria, for Lisbon, Évora and Faro, preventing the overheating risk with a lower cooling demand.

In order to adapt the PH concept for buildings in southern European warm climates, it is plausible to consider the maximum indoor air temperature limit 26 °C and therefore, this was chosen as the main criteria, using the descriptive statistics shown next. The results were statistically analysed and organised by region climate, shown in Table 7. The coefficient of variation (CV), mean and standard deviation of each set of parameters are included in the table.

Table 7. Statistical analysis of solutions.

		INPUTS																	
Case	Parameters	#00	#01	#02	#03 *	#04 *	#05	#06	#07	#08	#09	#10	#11	#12	#13	#14	#15	#16	#17 *
Bragança	m ± s	0.115	0.234	0.296	S6	S6	8.705	22.540	22.385	0.556	52.921	31.350	31.545	4.062	24.776	6.654	14.295	17.421	MVHR
		±	±	±			±	±	±	±	±	±	±	±	±	±	±	±	
	0.070	0.015	0.010	14.477			3.135	1.547	0.547	13.890	2.107	8.509	0.977	6.240	1.902	3.947	4.345		
	CV (%)	60.7	6.6	3.5			166.3	13.9	6.9	98.5	26.2	6.7	27.0	24.1	25.2	28.6	27.6	24.9	
Oporto	m ± s	0.194	0.238	0.298	S6	S6	5.019	22.389	21.190	1.752	37.357	24.538	23.063	3.793	23.670	5.799	13.658	13.901	MVHR
		±	±	±			±	±	±	±	±	±	±	±	±	±	±		
	0.049	0.007	0.008	0.083			0.846	0.478	0.088	3.322	3.837	2.249	0.690	4.149	0.845	2.171	2.417		
	CV (%)	25.1	2.8	2.6			1.7	3.8	2.3	5.0	8.9	15.6	9.8	18.2	17.5	14.6	15.9	17.4	
Aveiro	m ± s	0.196	0.239	0.299	S6	S6	5.010	22.484	21.279	1.675	47.944	17.013	26.420	3.619	23.336	5.839	20.320	13.218	MVHR
		±	±	±			±	±	±	±	±	±	±	±	±	±	±		
	0.051	0.003	0.003	0.084			0.895	0.440	0.151	9.460	1.671	5.721	0.583	3.532	1.182	3.318	1.992		
	CV (%)	25.9	1.1	0.9			1.7	4.0	2.1	9.0	19.7	9.8	21.7	16.1	15.1	20.2	16.3	15.1	
Lisbon	m ± s	0.166	0.212	0.286	S6	S6	7.692	23.544	22.044	1.288	54.447	31.467	36.276	3.683	25.836	9.214	19.218	16.258	MVHR
		±	±	±			±	±	±	±	±	±	±	±	±	±			
	0.031	0.058	0.022	7.617			1.977	0.992	0.272	5.644	1.749	2.842	0.249	3.850	0.805	1.131	1.414		
	CV (%)	18.9	27.4	7.6			99.0	8.4	4.5	21.1	10.4	5.6	7.8	6.8	14.9	8.7	5.9	8.7	
Évora	m ± s	0.142	0.221	0.285	S6	S6	5.608	22.875	21.813	1.046	44.490	31.662	31.869	4.107	33.669	6.940	16.501	19.777	MVHR
		±	±	±			±	±	±	±	±	±	±	±	±	±			
	0.055	0.040	0.024	3.210			1.414	1.218	0.622	10.257	1.063	8.380	0.902	7.310	1.782	3.728	3.232		
	CV (%)	38.9	18.3	8.3			57.2	6.2	5.6	59.5	23.1	3.4	26.3	22.0	21.7	25.7	22.6	16.3	
Faro	m ± s	0.085	0.224	0.294	S6	S6	7.100	22.485	22.191	1.587	52.307	31.558	30.419	4.056	26.478	9.455	14.252	13.587	MVHR
		±	±	±			±	±	±	±	±	±	±	±	±	±			
	0.038	0.045	0.013	11.183			1.421	1.438	0.327	11.044	0.935	5.950	0.624	5.447	1.030	2.436	2.462		
	CV (%)	44.9	20.3	4.5			157.5	6.3	6.5	20.6	21.1	3.0	19.6	15.4	20.6	10.9	17.1	18.1	

m—mean; s—standard deviation; CV—coefficient of variation; * For these variables the mode is presented.

One of the main features of the PH concept is the thermal building envelope defined with the purposes of reducing heat losses. Regarding the thermal insulation of the opaque envelope, high thickness of thermal insulation is fundamental as an average value close to the maximum allowed was attained for parameters #01 and #02. Concerning the insulation of the ground floor slab (#00), no clear trend was identified in the results, nor its dependence on the exterior climate. In fact, the variability of the insulation of the ground floor slab is related with the higher annual thermal amplitude, since higher values were found in cities with severe winter and summer. In colder climates, the insulation of walls (#01) is close to the maximum, while in warmer climates (Lisbon, Évora and Faro), more variability was observed, with the results pointing to higher CV. The maximum thickness was obtained for the roof insulation (#02), regardless of the location. There was a clear trend for window solutions (#03 and #04), with triple glazing windows (S6) for North and South orientation without significant variability between climates. Hence, the strongly insulated opaque envelope and double to triple glazing envelope is desirable, with the benefit of minimising the indoor air temperature asymmetry [46].

Regarding the shadings, the slat angle parameter (#05) tends to be low, which can be explained by an irrelevant importance of solar gains. Although, Bragança, Lisboa, Évora and Faro had higher values, with a slat angle at 90° positioned (closed) in some cases as they have a considerable CV. The activation temperature of blinds (#06) is relatively equal for all climate cases, observing a tendency to increase in hotter climates, with an ideal activation temperature about 22.5 °C for all climate regions.

The bypass activation temperature (#07) reveals no obvious relationship with climate severity. In addition, bypass air flow rate (#08) showed no clear relationship with climate regions, excluding the fact that there is a greater variability in climate regions with greater annual thermal amplitudes. The statistical results show no clear trend of the air change rate (#09 to #16) and a preference for the use of a ventilation system with heat recovery in relation to the common mechanical system (#17).

The statistical results reveal the need to have a strongly insulated thermal envelope and very good glazing solutions are needed to achieve the PH requirements for the Portuguese mainland. Other input parameters showed lower variability, demonstrating that these are stabilised values, leading to consensual choices for the designers. However, the input parameters allow a set of combinations of solutions (input parameters) for the input database meeting the PH compliance criteria. Although, an additional criterion, as an economic referee, is needed to simplify the options for the decision maker.

6. Life Cycle Costs Analysis

This section is an essential complement to the previously discussed descriptive statistical analysis of the best proposals. The main goal was to provide the building stakeholders and designers with the crucial information on which to base decision making. The multi-objective optimisation with differing objectives (two or more) results always range of optimum solutions and therefore, theoretically, it is not possible to define what solution is better than others. Introducing an additional criterion, besides the objective functions defined in the optimisation process, can be a successful strategy if one intends to achieve a single solution. Thus, by including an economic analysis, the authors attempt to identify the most cost-effective scenario from the set of Pareto optimum solutions. Traditionally, the result of an economic analysis is included in the multi-objective optimisation as an additional objective. However, the intention of this paper was to explore an alternative manner of taking into account this goal. With this approach, the relative importance given to this aspect is higher and it is possible to achieve a single optimum solution.

In this study, the investment evaluation was carried out using the LCC methodology developed for the analysis of energy conservation projects [47]. The LCC analysis was fulfilled evaluating three

types of cost: investment; operation and maintenance (O&M) and energy costs. Thus, to calculate the LCC of an energy conservation solution, the following Equation (3) was used [47]:

$$LCC = I + O\&M + E \quad (3)$$

In this equation, I is the present value (PV) of investment costs, $O\&M$ is the present value of operating and maintenance, and E is the energy costs present value.

The methodology requires the calculation of the present value of the entire cash flow throughout the period of analysis. A discount rate of 3% was chosen and the LCC analysis was carried out for a lifetime of 20 years. The energy related costs were calculated a price of 0.18 €/kW·h, with a corresponding annual escalation rate (e) of 0.20%.

The main objective of LCC analysis is to define an optimum solution from the solutions/results that define the Pareto front. This method was also implemented by the authors of Reference [27], using the economic optimisation as a decision factor, to select the best constructive solution amongst the dataset of the Pareto front. For the LCC calculations, the input data of variable investment includes the thermal insulation and the window solution prices. The remaining inputs used in the optimisation process have no influence over the investment cost. The installation cost of the variables investment is presented in Table 8.

Table 8. Installation costs of variable's investment input for life cycle cost (LCC) analysis.

Thickness (m)	Thermal Insulation		Solutions	Windows	
	Costs			Costs	
	Material/Application (€/m ²)	Maintenance (€/year)		Material/Application (€/m ²)	Maintenance (€/year)
0.00 to 0.03	5.09	7.01	S1	1815.26	27.22
0.04 to 0.07	9.34	7.67	S2	1760.69	28.19
0.08 to 0.11	15.28	8.67	S3	1721.07	26.07
0.12 to 0.15	23.20	10.30	S4	1699.89	23.38
0.16 to 0.19	28.86	11.65	S5	1674.23	24.48
0.20 to 0.23	35.65	12.85			
0.24 to 0.27	42.43	14.43	S6	2280.73	30.87
0.28 to 0.30	49.23	15.79			

The LCC analysis was carried out for all regions in the study. The LCC results are presented in Table 9. The lowest LCC values of the Pareto front solutions are shown in Table 9, highlighting the best solution (id#) and their variable's values separately for each climate regions. Faro, Évora and Lisbon are the regions with the lowest LCC values. The Aveiro region presents the highest LCC value, representing an increase of approximately 44% of the LCC value, when compared with Faro, the region with lowest LCC. The higher LCC values occur in the cities located in the north region, while the lowest LCC values occur in the south region cities with warmer climates.

Table 9. LCC results for the best Pareto front solutions for different climate regions.

City	Bragança	Oporto	Aveiro	Lisbon	Évora	Faro
Id./Variable	118	229	18	328	376	465
#00	0.061	0.096	0.146	0.126	0.080	0.060
#01	0.147	0.233	0.239	0.023	0.020	0.030
#02	0.263	0.277	0.300	0.280	0.300	0.270
#03 *	S6	S6	S6	S1	S2	S3
#04 *	S4	S5	S6	S1	S4	S6
#05	5.000	5.000	5.000	5.713	5.000	5.000

Table 9. Cont.

#06	21.000	22.576	22.070	22.401	21.000	21.000
#07	22.762	21.059	21.000	21.973	26.000	22.049
#08	1.241	1.749	1.649	1.280	1.800	1.800
#09	70.280	40.578	58.190	53.504	35.280	59.204
#10	32.040	29.975	15.840	29.942	32.040	31.409
#11	27.961	27.250	26.150	31.340	21.960	32.900
#12	5.400	3.131	2.911	3.607	2.880	4.613
#13	30.315	28.448	25.699	24.212	41.760	26.519
#14	7.011	5.050	5.084	8.822	5.040	10.080
#15	11.583	14.145	23.040	21.235	23.040	15.154
#16	13.994	14.633	11.520	16.219	23.040	11.520
#17 *	MVHR	MVHR	MVHR	MVHR	MVHR	MVHR
LCC (€)	73,275	78,857	84,407	63,289	63,783	58,862

* For these variables the mode is presented.

7. Conclusions

This study focuses on a dynamic thermal simulation of a light steel frame building using the EP software as a calculation engine. An evolutionary algorithm was used to calibrate the building energy model and to find the best constructive solutions and features of the active systems to fulfil the PH requirements for different regions of the Portugal mainland. Regarding the calibration process, the differences between real data and simulated results were minimised and the attained results allow us to conclude that the building energy model is calibrated according to the standards ASHRAE guideline 14 [37], IPMVP [38] and FEMP [39].

The constructive technology of lightweight steel frame construction offers a significant cost reduction compared to the traditional massive construction solutions and allows a higher quality control of construction procedures. However, the building technology studied herein presents a low thermal inertia and increased consequential risk of overheating [48]. The Passive House concept applied to lightweight constructive systems is viable for Portugal, however some adaptations of the constructive solutions are needed. The overheating risk obliges the use of simple upgrades in the constructive components and features, such as the use of automated blinds, to attain even better results with respect to the overheating reduction.

For southwest European climates, the overheating criteria imposed by the Passive House standard was not achieved for all climate regions of Portugal mainland and the adaptive comfort model is recommended. For some regions, an active cooling system is required, however, with low cooling demand to comply with the 25 °C criterion limit.

The features optimisation allowed the definition of several models that represent good solutions that comply with the Passive House requirements. However, stakeholders and designers must select the best solution that suits economic feasibility and high thermal comfort. Several best options are attained with two conflicting objectives, because there is no single dominated solution. Thus, a life cycle cost analysis was carried out to calculate the minimum life cycle cost value as a criterion of the decision to find and single out a best solution assuring the viability of the best combination designs. The methodology proposed in this study increases the energy efficiency of building construction, revealing a two-step approach to support decision making of the best building features to assure Passive House compliance criteria.

Author Contributions: Conceptualization, R.O., A.F., R.M.S.F.A. and R.V.; Methodology, R.O., A.F.; Software, R.O., A.F.; Validation, A.F., R.M.S.F.A. and R.V.; Formal Analysis, R.M.S.F.A., R.O.; Investigation, R.O.; Resources, A.F., R.V.; Writing—Original Draft Preparation, R.O.; Writing—Review & Editing, A.F., R.M.S.F.A. and R.V.; Visualization, R.O.; Supervision, A.F., R.M.S.F.A. and R.V.

Conflicts of Interest: The authors declare no conflicts of interest.

References

1. EPBD. Energy Performance of Buildings Directive 2010/31/EU (recast). In *Official Journal of the European Union*; European Commission: Brussels, Belgium, 2010; pp. 13–35.
2. ADENE. *Guia Da Eficiência Energética (Guide of Energy Efficiency)*; ADENE: Lisboa, Portugal, 2012; p. 94. (In Portuguese)
3. REH. Regulamento de Desempenho Energético de Edifícios de Habitação (Portuguese Regulation on the Energy Performance of Residential Buildings). In *Decree-Law No. 118/2013*; Diário Da República—1.ª Série—Nº 159; REH: Lisbon, Portugal, 2013. (In Portuguese)
4. RECS. Regulamento de Desempenho Energético dos Edifícios de Comércio e Serviços (Service Buildings Regulation). In *Decree-Law No. 118/2013*; Diário Da República—1.ª Série—Nº 159; RECS: Lisbon, Portugal, 2013. (In Portuguese)
5. IPCC. *Working Group III: Mitigation of Climate Change, Intergovernmental Panel on Climate*; IPCC: Geneva, Switzerland, 2014.
6. IEE. *Very Low-Energy House Concepts in North European Countries*; IEE (Intelligent Energy Europe): Brussels, Belgium, 2012.
7. PHI. *Passive House Institute*; PHI: Darmstadt, Germany, 2016.
8. Magnier, L.; Haghghat, F. Multiobjective optimization of building design using TRNSYS simulations, genetic algorithm, and Artificial Neural Network. *Build. Environ.* **2010**, *45*, 739–746. [[CrossRef](#)]
9. Kämpf, J.H.; Robinson, D. A simplified thermal model to support analysis of urban resource flows. *Energy Build.* **2007**, *39*, 445–453. [[CrossRef](#)]
10. Figueiredo, A.; Kämpf, J.; Vicente, R. Passive house optimization for Portugal: Overheating evaluation and energy performance. *Energy Build.* **2016**, *118*, 181–196. [[CrossRef](#)]
11. Crawley, D.B.; Hand, J.W.; Kummert, M.; Griffith, B.T. Contrasting the capabilities of building energy performance simulation programs. *Build. Environ.* **2008**, *43*, 661–673. [[CrossRef](#)]
12. Wang, W.; Zmeureanu, R.; Rivard, H. Applying multi-objective genetic algorithms in green building design optimization. *Build. Environ.* **2005**, *40*, 1512–1525. [[CrossRef](#)]
13. Tronchin, L.; Fabbri, K. Energy performance building evaluation in Mediterranean countries: Comparison between software simulations and operating rating simulation. *Energy Build.* **2008**, *40*, 1176–1187. [[CrossRef](#)]
14. Kämpf, J.H.; Wetter, M.; Robinson, D. A comparison of global optimization algorithms with standard benchmark functions and real-world applications using EnergyPlus. *J. Build. Perform. Simul.* **2010**, *3*, 103–120. [[CrossRef](#)]
15. Shorrock, L.; Dunster, J. The physically-based model BREHOMES and its use in deriving scenarios for the energy use and carbon dioxide emissions of the UK housing stock. *Energy Policy* **1997**, *25*, 1027–1037. [[CrossRef](#)]
16. Jones, P.J.; Williams, J.; Lannon, S. An energy and environmental prediction tool for planning sustainability in cities. In *Proceedings of the 2nd European Conference REBUILD*, Florence, Italy, 1–3 April 1998.
17. Robinson, D.; Campbell, N.; Gaiser, W.; Kabel, K.; Le-Mouel, A.; Morel, N.; Page, J.; Stankovic, S.; Stone, A. SUNtool—A new modelling paradigm for simulating and optimising urban sustainability. *Sol. Energy* **2007**, *81*, 1196–1211. [[CrossRef](#)]
18. Robinson, D.; Baker, N. Simplified modelling recent developments in the LT Method. *Build. Perform.* **2000**, *3*, 14–19.
19. Kämpf, J.H.; Robinson, D. A hybrid CMA-ES and HDE optimisation algorithm with application to solar energy potential. *Appl. Soft Comput.* **2009**, *9*, 738–745. [[CrossRef](#)]
20. Figueiredo, A.; Figueira, J.; Vicente, R.; Maio, R. Thermal comfort and energy performance: Sensitivity analysis to apply the Passive House concept to the Portuguese climate. *Build. Environ.* **2016**, *103*, 276–288. [[CrossRef](#)]
21. Figueiredo, A.; Kämpf, J.; Vicente, R.; Oliveira, R.; Silva, T. Comparison between monitored and simulated data using evolutionary algorithms: Reducing the performance gap in dynamic building simulation. *J. Build. Eng.* **2018**, *17*, 96–106. [[CrossRef](#)]
22. Figueiredo, A.; Vicente, R.; Lapa, J.; Cardoso, C.; Rodrigues, F.; Kämpf, J. Indoor thermal comfort assessment using different constructive solutions incorporating PCM. *Appl. Energy* **2017**, *208*, 1208–1221. [[CrossRef](#)]

23. Hasan, A.; Vuolle, M.; Siren, K. Minimisation of life cycle cost of a detached house using combined simulation and optimisation. *Build. Environ.* **2008**, *43*, 2022–2034. [[CrossRef](#)]
24. Badea, A.; Baracu, T.; Dinca, C.; Tutica, D.; Grigore, R.; Anastasiu, M. A life-cycle cost analysis of the passive house “POLITEHNICA” from Bucharest. *Energy Build.* **2014**, *80*, 542–555. [[CrossRef](#)]
25. Ekström, T.; Bernardo, R.; Blomsterberg, Å. Cost-effective passive house renovation packages for Swedish single-family houses from the 1960s and 1970s. *Energy Build.* **2018**, *161*, 89–102. [[CrossRef](#)]
26. Tokarik, M.S.; Richman, R.C. Life cycle cost optimization of passive energy efficiency improvements in a Toronto house. *Energy Build.* **2016**, *118*, 160–169. [[CrossRef](#)]
27. Almeida, R.M.S.F.; De Freitas, V.P. An insulation thickness optimization methodology for school buildings rehabilitation combining artificial neural networks and life cycle cost. *J. Civ. Eng. Manag.* **2016**, *22*, 915–923. [[CrossRef](#)]
28. European Committee for Standardization. *EN ISO 10211, Thermal Bridges in Building Construction. Heat Flows and Surface Temperatures—Detailed Calculations*; European Committee for Standardization: Brussels, Belgium, 2007; pp. 1–60.
29. European Committee for Standardization. *EN ISO 10077-1, Thermal Performance of Windows, Doors and Shutters—Calculation of Thermal Transmittance—Part 1: General*; European Committee for Standardization: Brussels, Belgium, 2006; Volume 1.
30. Kottek, M.; Grieser, J.; Beck, C.; Rudolf, B.; Rubel, F. World Map of the Köppen-Geiger climate classification updated. *Meteorol. Z.* **2006**, *15*, 259–263. [[CrossRef](#)]
31. IPMA, Instituto Português do Mar e da Atmosfera. 2017. Available online: www.ipma.pt (accessed on 1 February 2017).
32. Aguiar, R. *Clim. e Anos Meteorológicos de Referência para o Sist. Nac. de Certificação de Edifícios (versão 2013), Relatório Para ADENE—Agência de Energia*; Lisboa, I.P., Ed.; Laboratório Nacional de Energia e Geologia: Amadora, Portugal, 2013; Volume 55.
33. International Organization for Standardization. *EN ISO 7766, Ergonomics of the Thermal Environment, Instruments for Measuring Physical Quantities*; International Organization for Standardization: Geneva, Switzerland, 1998.
34. Cipriano, J.; Mor, G.; Chemisana, D.; Pérez, D.; Gamboa, G.; Cipriano, X. Evaluation of a multi-stage guided search approach for the calibration of building energy simulation models. *Energy Build.* **2015**, *87*, 370–385. [[CrossRef](#)]
35. Passive-On. *The Passivhaus Standard in European Warm Climates: Design Guidelines for Comfortable Low Energy Homes*; Efficiency Research Group of Polytechnic of Milan: Milan, Italy, 2006.
36. Vidal, F.; Meireles, I.; Vicente, R.; Sousa, V.; Rodrigues, F. Thermal comfort performance of a passive house in summer under a Mediterranean climate. In Proceedings of the 41st IAHS World Congress—Sustainability Innovation for the Future, Albufeira, Portugal, 13–16 September 2016.
37. ASHRAE. ASHRAE Guideline 14-2002 Measurement of Energy and Demand Savings, American Society of Heating, Refrig. Air-Cond. Eng. **2002**, *8400*, 170.
38. IPMVP. *International Performance Measurement and Verification Protocol, Concepts and Options for Determining Energy and Water Savings*; International Performance Measurement and Verification Protocol Committee: Washington, DC, USA, 2002; Volume 1.
39. FEMP, US DOE. *M&V Guidelines: Measurement and Verification for Federal Energy Projects Version 3.0, Federal Energy Management Program*; US Department of Energy: Washington, DC, USA, 2008.
40. Bou-Saada, T.E.; Haberl, J.S. *An Improved Procedure for Developing Calibrated Hourly Simulation Models*; IBPSA-USA: Washington, MI, USA, 1995.
41. Kreider, J.F.; Haberl, J.S. Predicting hourly building energy usage. *ASHRAE J.* **1994**, *36*, 6.
42. Kreider, J.F.; Haberl, J.S. Predicting hourly building energy use: The great energy predictor shootout: Overview and discussion of results. *ASHRAE Trans. Res.* **1994**, *100*, 1104–1118.
43. European Committee for Standardization. *EN 15251, Indoor Environmental Input Parameters for Design and Assessment of Energy Performance of Buildings Addressing Indoor Air Quality, Thermal Environment, Lighting and Acoustics*; European Committee for Standardization: Brussels, Belgium, 2007.
44. Wu, Z.; Xia, X.; Wang, B. Improving building energy efficiency by multiobjective neighborhood field optimization. *Energy Build.* **2015**, *87*, 45–56. [[CrossRef](#)]

45. Schnieders, J.; Feist, W.; Rongen, L. Passive Houses for different climate zones. *Energy Build.* **2015**, *105*, 71–87. [[CrossRef](#)]
46. Feist, W.; Schnieders, J.; Dorer, V.; Haas, A. Re-inventing air heating: Convenient and comfortable within the frame of the Passive House concept. *Energy Build.* **2005**, *37*, 1186–1203. [[CrossRef](#)]
47. Fuller, S.K.; Petersen, S.R. *NIST Handbook 135: Life-Cycle Costing Manual for the Federal Energy Management Program*; National Institute of Standards and Technology: Gaithersburg, MD, USA, 1996; Volume 5.
48. Santos, P.; Gervásio, H.; da Silva, L.S.; Lopes, A.G. Influence of climate change on the energy efficiency of light-weight steel residential buildings. *Civ. Eng. Environ. Syst.* **2011**, *28*, 325–352. [[CrossRef](#)]



© 2018 by the authors. Licensee MDPI, Basel, Switzerland. This article is an open access article distributed under the terms and conditions of the Creative Commons Attribution (CC BY) license (<http://creativecommons.org/licenses/by/4.0/>).